

# THE CRYSTALLOGRAPHY AND TEXTURE OF Co-BASED THIN FILM DEPOSITED ON Cr UNDERLAYERS

David E. Laughlin  
Dept. of Metallurgical Engineering  
and Materials Science  
Carnegie Mellon University  
Pittsburgh, PA 15213.

Bunsen Y. Wong  
Dept. of Metallurgical Engineering  
and Materials Science  
Carnegie Mellon University  
Pittsburgh, PA 15213.

## ABSTRACT

Various Co-based alloys (*hcp*) have been developed for use as longitudinal magnetic recording media. Many investigators have found that the use of Cr underlayers (*bcc*) greatly affects the magnetic properties of the films. Several investigators have related this to the effect of the Cr underlayer on the crystallographic texture of the thin magnetic Co-based films. In this review paper some of the evidence for the effect of Cr orientation on the crystallographic orientation of Co-based thin films is presented. This evidence is based on x-ray diffraction, selected area electron diffraction, electron micro-diffraction of the Co/Cr bi-layer film and atomic resolution electron microscopy of cross sections of the bi-layer films. We show that a {110} Cr surface gives rise to a {10 $\bar{1}$ 1} type Co-based alloy thin film texture, whereas a {200} Cr surface produces a {1120} type Co-based alloy thin film texture.

It has been nearly a quarter of a century since the discovery that a Cr underlayer increases the in-plane magnetic coercivity of sputtered Co based alloy thin films [1,2]. One of the proposed mechanisms for this increase in coercivity is the supposition that the Cr underlayer produces a Co film with a preferred crystallographic orientation [3,4]. In a previous paper we reviewed some of the evidence for crystallographic texture in these thin films [5]. In this paper we review four experimental techniques that can be used to investigate the orientation relationships (OR) between the magnetic Co-based film and the Cr underlayer. These techniques are x-ray diffraction, selected area (electron) diffraction (SAD), electron microdiffraction ( $\mu$ D) and atomic resolution electron microscopy.

Figure 1 is a schematic drawing showing the important components of a thin film disk for magnetic recording. Of interest to us in this review is the crystallographic orientation relationships between the grains in the magnetic film and those in the Cr (*bcc*) underlayer. The magnetic films which we discuss will all be alloys of Co, usually with the *hcp* structure. Hence, the OR's of interest to us are those between *hcp* and *bcc*. Since certain interplanar spacings in Co and Cr have nearly the same values, a special set of OR's are established during the deposition process of the Co-based alloy onto the Cr underlayer.

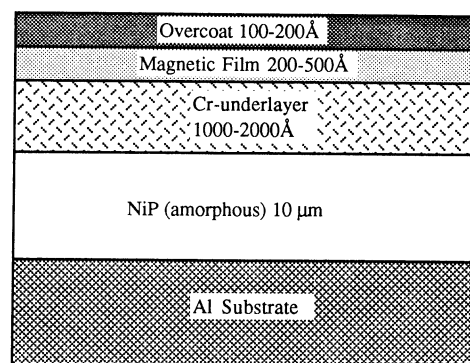


Figure 1. A schematic drawing of the various layer in a hard disk

We start with a brief review of the important planes in the *bcc* and *hcp* structures. Figure 2(a) shows the two types of planes of Cr which are most likely to be parallel to the thin film surface, namely the {200} and {110} planes. The {110} planes are the closest-packed planes for the *bcc* structure, and in the case of Cr films are the ones which are most likely to lie parallel to the film surface when the films are grown without substrate heating [6]. When deposited at elevated temperatures (>150°C) the {200} texture is commonly observed [7-10]. The figures shown in 2(b) highlight the hexagonal close packed structure (*hcp*) and several of its important crystallographic directions and planes. Here the (0002) planes are close packed ones. Notice that if the (01 $\bar{1}$ 0) or (1120) planes are parallel to the plane of the film, the *c* axis will be in the plane of the film. However, if (01 $\bar{1}$ 1) is in the plane of the film, the *c* axis will be at an angle of 28° with respect to the film surface. Also note that if the (0002) plane is parallel to the plane of the film the *c* axis is perpendicular to the film surface.

Before we discuss the methods that we have used to investigate the crystallographic OR between thin films of Co on Cr we give a brief summary of important concepts of diffraction from thin films.

For diffraction to occur from a thin film, the well known Bragg Law must be satisfied.

$$\lambda = 2d \sin\theta$$

where  $\lambda$  is the wavelength of the radiation,  $d$  is the interplanar spacing and  $\theta$  is the Bragg angle. When using x-rays, the radiation wavelength is of the order of magnitude of the

Presented at IEEE/Intermag Conference June 18-21, 1991. This review is based on research supported in part by the NSF under Grant No. ECD-8907068 and by the DOE under Grant No. DE-FG02-90-ER45423. The government has certain rights in this material.

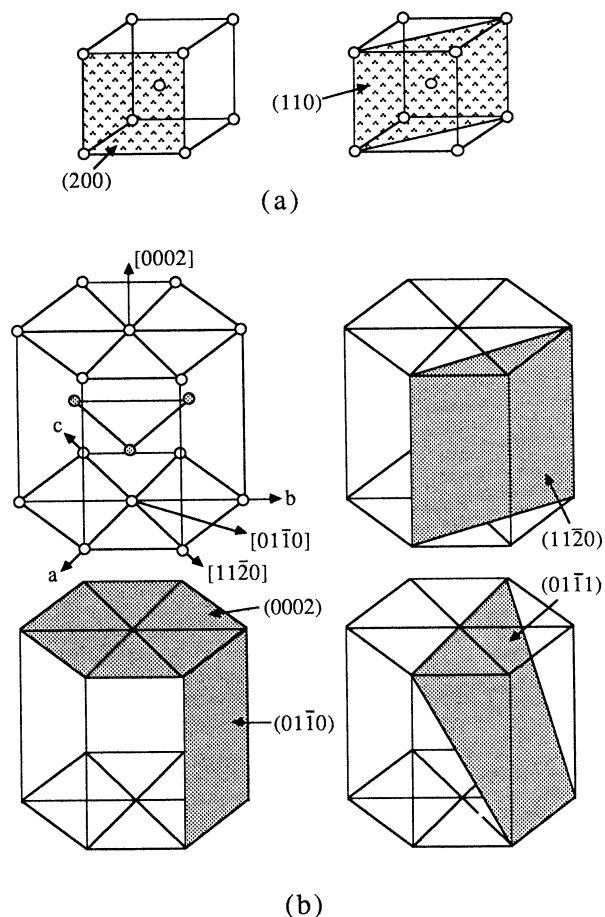


Figure 2. Schematic drawing of the low index planes and directions in (a) bcc and (b) hcp.

crystallographic interplanar spacings ( $\sim \text{\AA}$ ). This means that the Bragg angles will be in the range of  $15\text{--}60^\circ$ . When studying films by x-ray diffraction in the symmetrical reflection mode, it is those planes which are parallel to the film surface that give rise to the strongest reflections (see Figure 3). On the other hand, the Bragg angles for electron diffraction, when using the transmission mode, are nearly  $0^\circ$ , because the wavelength of the electrons is usually much smaller than the  $d$  spacing of the crystals. Thus, the planes which diffract are those that are nearly perpendicular to the plane of the film (see Figure 3). In crystallographic terminology, the planes which diffract in transmission electron diffraction are the planes of the zone axis  $[uvw]$  where  $[uvw]$  is the direction of the electron beam in terms of the crystallographic axes of the thin film. It is important to keep these geometric relationships in mind when interpreting diffraction results. For example if the  $(0002)$  planes of an hcp structure are parallel to the plane of the film, they will be diffracted strongly by x-rays utilizing the symmetric diffraction mode shown in Figure 3, but will not be present in the transmission electron diffraction patterns. On the other hand if the  $c$ -axis is in the plane of the film, the  $(0002)$  planes will diffract in the TEM mode, but will not be diffracted by x-rays in the symmetric reflection mode.

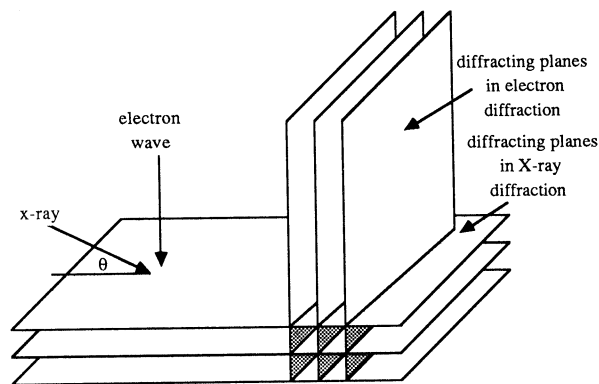


Figure 3. The Bragg angle in electron diffraction is very small and the diffracting planes are almost parallel to the direction of the electron beam. In X-ray diffraction, however, the Bragg angle is much larger and the planes which diffract are those parallel to the plane of the film.

We now review some information about the diffraction patterns of Cr and *hcp* Co. We will first discuss the *bcc* structure.

As is well known, the *bcc* structure is based on the *bcc* Bravais Lattice, with an atom at each Bravais Lattice point. The Space Group of the structure is  $\text{Im}\bar{3}\text{m}$ , its Pearson Symbol is  $\text{cI}2$  and its lattice parameter is  $2.88 \text{ \AA}$ . The structure factors for the various planes are given as:

$$\begin{aligned} F &= 2f \quad \text{for } h+k+l = \text{even} \\ F &= 0 \quad \text{for } h+k+l = \text{odd} \end{aligned}$$

where  $f$  is the atomic scattering factor for the radiation being used. For x-ray diffraction, using  $\text{CuK}\alpha$  radiation ( $\lambda = 1.54 \text{ \AA}$ ), the first several reflections from *bcc* Cr are as follows: [11]

$hkl$	$2\theta$
{110}	44.2
{200}	64.1
{211}	81.7
{220}	98.1

Experiments to date have found two different crystallographic textures for Cr films: namely those with a {100} texture and those with a {110} texture (see for example [5]). These textures give rise to strong {200} and {110} x-ray reflections respectively.

The Co based alloys that are most commonly used for thin film recordings include Co-Ni-Cr, Co-Cr-Ta, Co-Ni-Pt, etc. They have the *hcp* structure, based on the primitive hexagonal Bravais Lattice, with two atoms per Bravais Lattice point. The Space Group for the *hcp* structure is  $\text{P6}_3/\text{mmc}$ , and the Pearson symbol of the structure is  $\text{hP}2$ .

For our discussion we will use the values of  $c$  and  $a$  for Co-Ni-Cr which we determined by X-ray diffraction, viz.  $c=4.07\text{\AA}$ ,  $a=2.50\text{\AA}$ . It should be kept in mind that the exact positions of the reflections will vary for each of the specific Co alloys although the differences are small. The structure factor conditions for *hcp* are: [11]

$h+2k$	1	$ F ^2$
3m	odd	0
3m	even	$4f^2$
3m+1	odd	$3f^2$
3m+1	even	$f^2$

where  $m$  is an integer. Thus the first several x-ray reflections from Co-Ni-Cr ( $a=2.50$  and  $c=4.07$ ) are:

$(hk\cdot l)$	$2\theta^\circ$
{1010}	41.8
{0002}	44.7
{1011}	47.6
{1012}	62.8
{1120}	76.2
{1013}	84.4

It can be noted immediately that the {0002} reflection for Co is very close in position to the {110} reflection for Cr (44.7 vs. 44.2).

An example of a x-ray diffraction pattern of a hard disk is shown in Figure 4. This was taken in the symmetrical reflection mode, using a monochromator. The prominent peaks are from the Al substrate (labeled) and the amorphous NiP layer (broad peak centered at  $\sim 45^\circ 2\theta$ ). This demonstrates that it is very difficult to observe the reflections from Cr or the Co-based thin films when the films are on the disks. This is especially so in the region of  $2\theta \approx 45^\circ$ , where the {0002}<sub>Co</sub> and {110}<sub>Cr</sub> reflections should appear. The crystallographic information is more easily obtained by electron diffraction. This is discussed below.

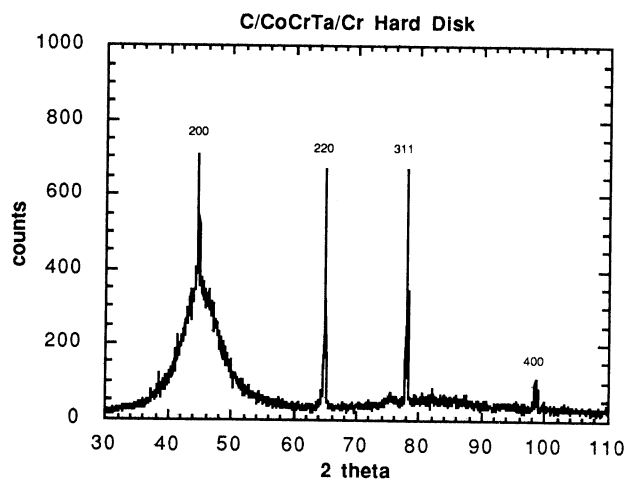


Figure 4. X-ray diffraction spectrum of CoCrTa/Cr/NiP/Al hard disk. The peaks are Al (200), (220), (311) and (400) respectively. The broadening at the base of the (200) peak is due to the amorphous NiP.

An alternative way of studying the crystallography of Co-alloy on Cr thin films by x-ray diffraction is to sputter the films directly onto glass substrates. The x-ray spectrum for such a bi-layer is shown in Figure 5. This spectrum was taken using a monochromator. The film was sputtered with a substrate temperature of about  $260^\circ\text{C}$ . The reflection near  $44.5^\circ$  is labeled as the {0002}<sub>Co</sub> of CoNiCr and {110} of Cr. The large reflection near  $64^\circ$  is the {200} of Cr. This shows that this Cr film has a strong {200} texture. The CoNiCr {1120} reflection demonstrates that these planes must be in the plane of the film. As discussed above, this means that the  $c$  axis lies in the film plane. See Figure 2(b). From this pattern it can be deduced that the {1120} planes of Co are parallel to the {200} planes of Cr.

A second method of studying the crystallographic texture of the thin films is by transmission electron microscopy. In selected area diffraction (SAD), a parallel beam of electrons impinges on an area of the sample of the order of microns in diameter. A diffraction pattern forms in the back focal plane of the objective lens. For films with grain sizes of the order of  $200\text{\AA}$ , the diffraction pattern is actually the superposition of many patterns, forming the well known ring patterns. Figure 6 shows schematics for ring patterns for *bcc* Cr and *hcp* CoNiCr. In Figure 6(a), the "ring pattern" for a random array of *bcc* Cr grains is displayed. All the "rings" are present. Figure 6(b) shows the pattern that would be produced if all the grains have {100} planes parallel to the film plane. In this case the {112} ring would be missing since no {112} plane would be perpendicular to the film surface. Figure 6(c) is a schematic of the ring pattern for a random array of *hcp* grains. For an *hcp* film with {0001} texture, the {0002} ring would be missing, as would the  $(10\bar{1}1), (10\bar{1}2) \dots [hk\cdot l]$  rings where  $l \neq 0$ . Figure 6(d) is the superpositioning of the *hcp* and *bcc* ring patterns.

Figure 7 is a typical SAD pattern from a bi-layer thin film of CoNiCr on Cr. In comparing the positions of each of the rings with the schematic shown in Figure 6(d), it can be seen that no strong crystallographic texture exists in this film. Of course, the relative intensities must also be compared before it can be stated unequivocally that the films are completely random in orientation. Hono *et al.* [5] have calculated the relative intensities for electron diffraction from thin films with various textures.

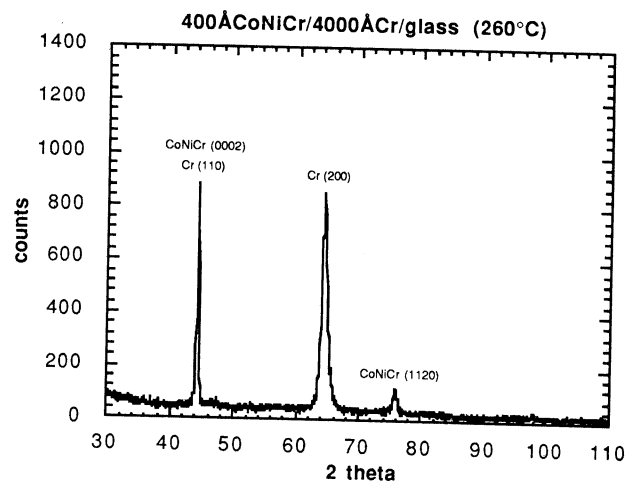


Figure 5. X-ray diffraction spectrum of CoNiCr/Cr/glass bi-layer thin films.

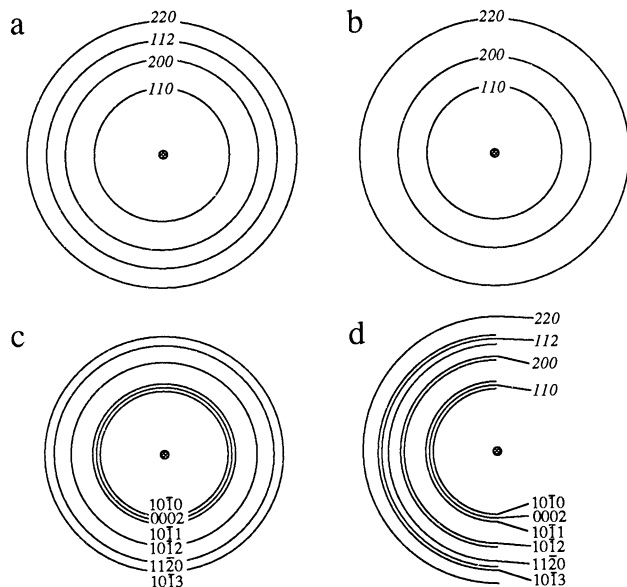


Figure 6. Schematic drawings of the SAD patterns of (a) bcc Cr, (b) [100] texture bcc Cr, (c) hcp CoNiCr and (d) hcp CoNiCr/bcc Cr bi-layer thin films.

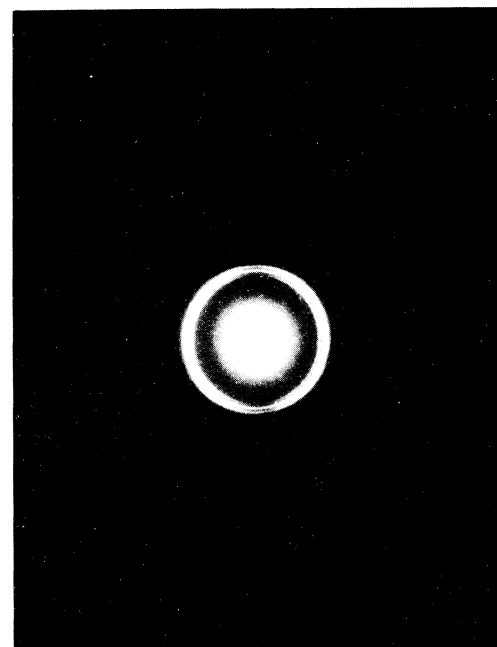


Figure 7. SAD Pattern of a CoNiCr/Cr bi-layer thin film

The x-ray and SAD techniques look at the diffraction patterns produced by many grains. We turn now to two techniques that investigate the orientation of one grain of CoNiCr with respect to one grain of the Cr underlayer.

An electron microdiffraction pattern ( $\mu$ D) is produced when a convergent beam of electrons impinges on the film. Thus, even for grain sizes as small as 200 Å, if the beam is converged to a size of about 100 Å, the resulting diffraction pattern can be thought of as arising from an individual grain. Such patterns are displayed in Figure 8.

Figure 8 displays two different OR's between CoNiCr and Cr. In 8(a), the Cr pattern is seen to be from an [001] zone axis. This means that the Cr plane parallel to the film surface is the (001) plane. The zone axis of the superposed *hcp* pattern is  $[11\bar{2}0]$ . This means that the  $(11\bar{2}0)$  plane of CoNiCr is parallel to the film surface and thus parallel to the (001) Cr plane. From the microdiffraction patterns we also see that the (0002) CoNiCr plane is parallel to the (110) Cr plane. Hence the OR is the Pitsch-Schrader OR [12]. The patterns shown in 8(b) display the Potter OR [13]. This is the one which occurs when the Cr texture is (110). In this case the *c* axis of the hexagonal alloy is  $28^\circ$  from the plane of the film. See [5] and [14] for other OR's obtained by microdiffraction.

The last technique to be discussed is that of atomic resolution transmission electron microscopy. In order to see OR across the interface, it is necessary to prepare cross-sectional specimens. Figure 9 shows the interface between CoNiCr and Cr for the case when the (001) plane of Cr is parallel to the surface of the film, as is the  $(11\bar{2}0)$  plane of CoNiCr [15]. This is the Pitsch-Schrader OR. This photograph was taken along the  $[110]$  zone for Cr and along the  $[0001]$  zone for the *hcp* CoNiCr. The micrograph reveals that (110) planes of Cr (lower part of diagram) and the  $(11\bar{0}0)$  planes of Co are parallel to each other. Close examination of the interface reveals that there are regions of good fit, as well as regions that are not perfectly matched. The details of such micrographs are currently being investigated in our laboratory.

## CONCLUSION

We have reviewed and summarized four techniques to investigate the OR across the interface of bi-layer Co-based/Cr thin films. These techniques are complementary to each other. By using them over the past several years we have documented several OR's between Co based alloys and Cr thin films enabling us to better understand the factors which control the crystallographic texture of the magnetic thin films.

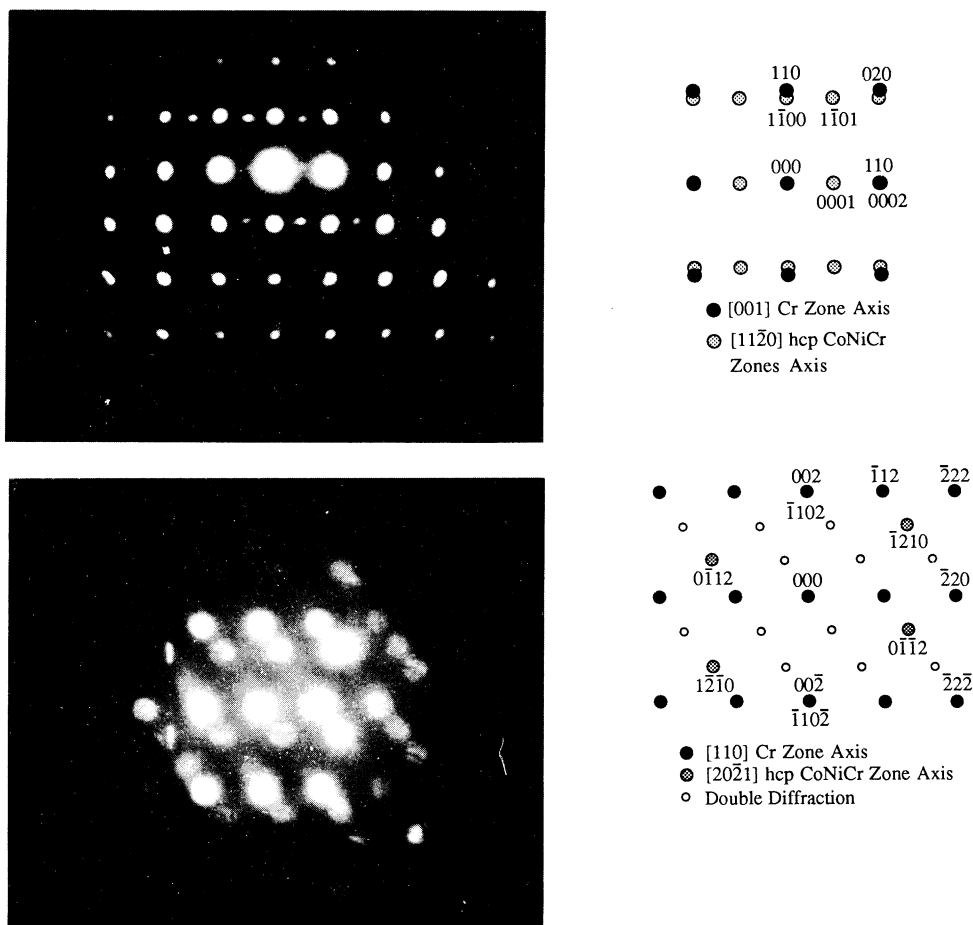


Figure 8. Microdiffraction patterns revealing the grain to grain O.R. in CoNiCr/Cr bi-layer thin films. The O.R. is (a) Pitsch-Schrader when the Cr surface has a (100) orientation and (b) Potter when the orientation is (110).

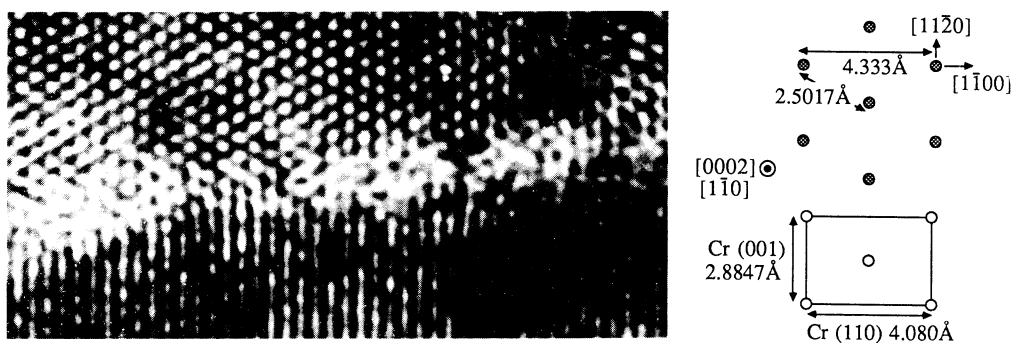


Figure 9. HRTEM image of the interface between CoNiCr and Cr. The O.R. is that of Pitsch-Schrader.

#### REFERENCES

- [1] J.P. Lazzari, I. Melnick and D. Randet, IEEE Trans. Magn., Vol. , 205 (1967).
- [2] J.P. Lazzari, I. Melnick and D. Randet, IEEE Trans. Magn. Vol. 5, 955 (1969).
- [3] H.J. Lee, J. Appl. Phys., Vol. 63, 3269 (1988).
- [4] T. Ohno, Y. Shiroishi, S. Hishiyama, H. Suzuki and Y. Matsuda, IEEE Trans. Magn., Vol. 23, 2809 (1989).
- [5] K. Hono, B. Wong and D.E. Laughlin, J. Appl. Phys., Vol. 68(9), 4734 (1990).
- [6] S.L. Duan, J.O. Artman, B. Wong and D.E. Laughlin, IEEE Trans. Magn., Vol. 26(5), 1587 (1990).
- [7] S.L. Duan, J.O. Artman, J-W. Lee, B. Wong and D.E. Laughlin, IEEE Trans. Magn., Vol. 25(5), 3884 (1989).
- [8] S.L. Duan, J.O. Artman, J-W. Lee, B. Wong and D.E. Laughlin, J. Appl. Phys., Vol. 67(9), 4913 (1990).
- [9] J.K. Howard, R. Ahlert and G. Lim, J. Appl. Phys., Vol. 61(8), 3834 (1987).
- [10] K.E. Johnson, P.R. Ivett, D.R. Timmons, M. Mirzamdani, S.E. Lambert and T. Yogi, J. Appl. Phys., Vol. 67(9), 4686 (1990).
- [11] B.D. Cullity, Elements of X-ray Diffraction, second edition, Addison-Wesley Publishing Co (1978).
- [12] W. Pitsch and A. Schrader, Arch. Eisenhütt Wes., Vol. 29, 715 (1958).
- [13] W. Potter, J. Less-Common Metals, Vol. 31, 299 (1973).
- [14] T. Yogi, G.L. Gorman, C. Hwang, M.A. Kakalec and S.E. Lambert, IEEE Trans. Magn., Vol. 24(6), 2727 (1988).
- [15] B. Wong and D.E. Laughlin, "A HRTEM investigation of CoNiCr/Cr thin films," to be published in Proceedings of 49th Annual Meeting of the Electron Microscopy Society of America (EMSA/MAS Meeting, San Jose, CA, 1991), W. Bailey, Editor, San Francisco Press.